Comparison of Excited-State Energy Transfer in Arrays of Hydroporphyrins (Chlorins, Oxochlorins) versus Porphyrins: Rates, Mechanisms, and Design Criteria

Masahiko Taniguchi,[†] Doyoung Ra,[†] Christine Kirmaier,[‡] Eve Hindin,[‡]
Jennifer K. Schwartz,[‡] James R. Diers,[§] Robert S. Knox,[*,ǁ] David F. Bocian,[*,§]
Jonathan S. Lindsey,[*,†] and Dewey Holten[*,‡]

*Contribution from the Department of Chemistry, North Carolina State University,
Raleigh, North Carolina 27695-8204, Department of Chemistry, Washington University,
St. Louis, Missouri 63130-4889, Department of Chemistry, University of California,
Riverside, California 92521-0403, and Department of Physics and Astronomy,
University of Rochester, Rochester, New York 14627-0171*

Received May 6, 2003; E-mail: holten@wuchem.wustl.edu

Abstract: A set of chlorin−chlorin and oxochlorin−oxochlorin dyads has been prepared with components in the same or different metalation states. In each case a 4,4′-diphenylethyne linker spans the respective 10-position of each macrocycle. The dyads have been studied using static and time-resolved absorption and emission spectroscopy, resonance Raman spectroscopy, and electrochemical techniques. Excited-state energy transfer from a zinc chlorin to a free-base (Fb) chlorin occurs with a rate constant of $(110 \text{ ps})^{-1}$ and an efficiency of 93%; similar values of $(140 \text{ ps})^{-1}$ and 83% are found for the corresponding oxochlorin dyad. Energy transfer in both dyads is slower and less efficient than found previously for the analogous porphyrin dyad, which displays a rate of $(24 \text{ ps})^{-1}$ and a yield of 99%. The slower rates and diminished efficiencies in the ZnFb chlorin and oxochlorin dyads versus the ZnFb porphyrin dyad are attributed to substantially weaker linker-mediated through-bond (TB) electron-exchange coupling (as indicated by resonance Raman data). Although the through-space (TS, i.e., dipole−dipole) coupling in the ZnFb-chlorin and -oxochlorin dyads is enhanced relative to the ZnFb porphyrin dyad (as indicated by Förster calculations), this enhancement is insufficient to compensate for the greatly diminished TB coupling. Taken together, the chlorin and oxochlorin dyads examined herein serve as benchmarks for elucidating the energy-transfer, electrochemical, and other properties of light-harvesting arrays containing multiple chlorins or oxochlorins.

Introduction

Porphyrins have served as the principal building blocks for the construction of a wide variety of synthetic multicomponent light-harvesting arrays.[1] The use of hydroporphyrins in such constructs has been limited by comparison. Hydroporphyrins are structurally more similar to natural photosynthetic pigments than are porphyrins, and these structural features impart important photophysical properties to the molecules. In particular, hydroporphyrins contain one (or more) saturated pyrrole rings. Pyrrole-ring saturation results in a greatly enhanced oscillator strength in the long-wavelength absorption relative to porphyrins.[2] A second effect of pyrrole-ring saturation is that hydroporphyrins are linear oscillators whereas metalloporphyrins are planar oscillators.[3] The enhanced oscillator strength in the long-wavelength absorption of hydroporphyrins affords enhanced through-space (TS) coupling between constituents in multichromophoric arrays. An important issue is whether these properties transform into more rapid and efficient energy flow to a trap site in light-harvesting arrays constructed from hydroporphyrins compared to analogous porphyrin-based architectures.

Hydroporphyrin dyads provide benchmarks for assessing the extent of electronic communication and the rates and efficiencies of energy transfer between the constituent components of multichromophoric arrays. A number of covalently linked dyads containing chlorins or oxochlorins have been prepared for studies in photodynamic therapy or as models of the photosynthetic special pair,[4] but only a few hydroporphyrin dyads have

[†] North Carolina State University.

[‡] Washington University.

[§] University of California.

[ǁ] University of Rochester.

(1) (a) Harvey, P. D. In *The Porphyrin Handbook*; Kadish, K. M., Smith, K. M., Guilard, R., Eds.; Academic Press: San Diego, CA, 2003; Vol. 18, pp 63−250. (b) Burrell, A. K.; Officer, D. L.; Plieger, P. G.; Reid, D. C. W. *Chem. Rev.* **2001**, *101*, 2751−2796.

(2) Smith, J. H. C.; Benitez, A. In *Modern Methods of Plant Analysis*; Paech, K., Tracey, M. V., Eds.; Springer-Verlag: Berlin, 1955; Vol. IV, pp 142−196.

(3) (a) Gurinovich, G. P.; Sevchenko, A. N.; Solov'ev, K. N. *Opt. Spectrosc.* **1961**, *10*, 396−401. (b) Gouterman, M.; Stryer, L. *J. Chem. Phys.* **1962**, *37*, 2260−2266.

(4) (a) Wasielewski, M. R. *Chem. Rev.* **1992**, *92*, 435−461. (b) Wasielewski, M. R. In *Chlorophylls*; Scheer, H., Ed.; CRC Press: Boca Raton, FL, 1991; pp 269−286.

been examined for energy transfer.[5] Each of the latter employs derivatives of chlorophylls and bacteriochlorophylls. No studies have been made to compare the energy-transfer properties of analogous hydroporphyrin dyads and porphyrin dyads. A chief obstacle may lie in the lack of adequate synthetic strategies for preparing hydroporphyrin dyads in defined architectures that contain macrocycles in distinct metalation states.
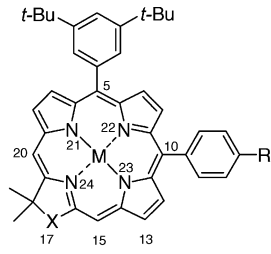
Recently, we developed a rational synthesis of chlorins that enables the facile preparation of 100-mg quantities of chlorin building blocks.[6-8] Furthermore, oxidation of the chlorins affords ready access to regioisomerically pure oxochlorins.[9] Oxochlorins have approximately the same spectral properties as chlorins but exhibit oxidation potentials resembling those of porphyrins. The availability of chlorin and oxochlorin building blocks has enabled us to prepare a set of the corresponding dyads. Herein, we describe the synthesis of chlorin—chlorin and oxochlorin—oxochlorin dyads with components in the same or different metalation states and examine the photophysical properties of these dyads. These studies address the fundamental question of the efficacy of analogous hydroporphyrin versus porphyrin arrays for light-harvesting and excited-state energy flow and provide basic information needed for the rational design and construction of larger chlorin- and oxochlorin-based light-harvesting arrays.

Results

Synthesis of Chlorin—Chlorin and Oxochlorin—Oxochlorin Dyads. We initially attempted to synthesize chlorin—chlorin dyads wherein each chlorin incorporated a *p*-tolyl group at one nonlinking *meso*-position; however, the dyads exhibited low solubility in organic solvents. We turned to the use of a 3,5-di-*tert*-butylphenyl group at the nonlinking 5-position to afford greater solubility of the chlorin building block and the corresponding dyads. The requisite *meso*-substituted chlorins were prepared, each bearing one 3,5-di-*tert*-butylphenyl group at the 5-position and either an iodophenyl group or an ethynylphenyl group at the 10-position (**Zn1**, **Zn2**)[8] (Chart 1). The required *meso*-substituted oxochlorins (**Oxo-Zn1**, **Oxo-Zn2**) were prepared by oxidation of the corresponding chlorin at the 17-position using basic alumina and DDQ.[9] The free-base chlorin and oxochlorin building blocks (**1**, **2**, **Oxo-1**, and **Oxo-2**) were obtained by demetalation of the corresponding Zn chelates with TFA.[9] The Cu chelates of chlorin and oxochlorin building blocks (**Cu1**, **Cu2**, **Oxo-Cu1,** and **Oxo-Cu2**) were prepared by treating the free-base species with Cu(OAc)$_2$.[9]
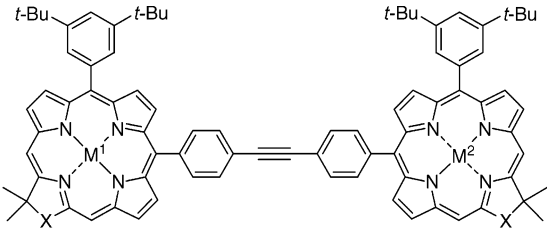
The coupling of iodo-substituted and ethyne-substituted chlorin or oxochlorin building blocks was performed using the standard Pd-mediated conditions that have been developed for joining porphyrins. These conditions employ Pd$_2$(dba)$_3$ and P(*o*-tol)$_3$ in toluene/TEA (5:1) in dilute solution (2.5 mM equimolar

(5) (a) Tamiaki, H.; Miyatake, T.; Tanikaga, R.; Holzwarth, A. R.; Schaffner, K. *Angew. Chem., Int. Ed. Engl.* **1996**, *35*, 772−774. (b) Osuka, A.; Marumo, S.; Wada, Y.; Yamazaki, I.; Yamazaki, T.; Shirakawa, Y.; Nishimura, Y. *Bull. Chem. Soc. Jpn.* **1995**, *68*, 2909−2915. (c) Osuka, A.; Wada, Y.; Maruyama, K.; Tamiaki, H. *Heterocycles* **1997**, *44*, 165−168.
(6) (a) Strachan, J.-P.; O'Shea, D. F.; Balasubramanian, T.; Lindsey, J. S. *J. Org. Chem.* **2000**, *65*, 3160−3172. (b) Strachan, J.-P.; O'Shea, D. F.; Balasubramanian, T.; Lindsey, J. S. *J. Org. Chem.* **2001**, *66*, 642.
(7) Balasubramanian, T.; Strachan, J. P.; Boyle, P. D.; Lindsey, J. S. *J. Org. Chem.* **2000**, *65*, 7919−7929.
(8) Taniguchi, M.; Ra, D.; Mo, G.; Balasubramanian, T.; Lindsey, J. S. *J. Org. Chem.* **2001**, *66*, 7342−7354.
(9) Taniguchi, M.; Kim, H.-J.; Ra, D.; Schwartz, J. K.; Kirmaier, C.; Hindin, E.; Diers, J. R.; Prathapan, S.; Bocian, D. F.; Holten, D.; Lindsey, J. S. *J. Org. Chem.* **2002**, *67*, 7329−7342.

Compound	X	M	R
Zn1	CH$_2$	Zn	ethyne
Zn2	CH$_2$	Zn	I
1	CH$_2$	H, H	ethyne
2	CH$_2$	H, H	I
Cu1	CH$_2$	Cu	ethyne
Cu2	CH$_2$	Cu	I
Oxo-Zn1	C=O	Zn	ethyne
Oxo-Zn2	C=O	Zn	I
Oxo-1	C=O	H, H	ethyne
Oxo-2	C=O	H, H	I
Oxo-Cu1	C=O	Cu	ethyne
Oxo-Cu2	C=O	Cu	I

Chart 2

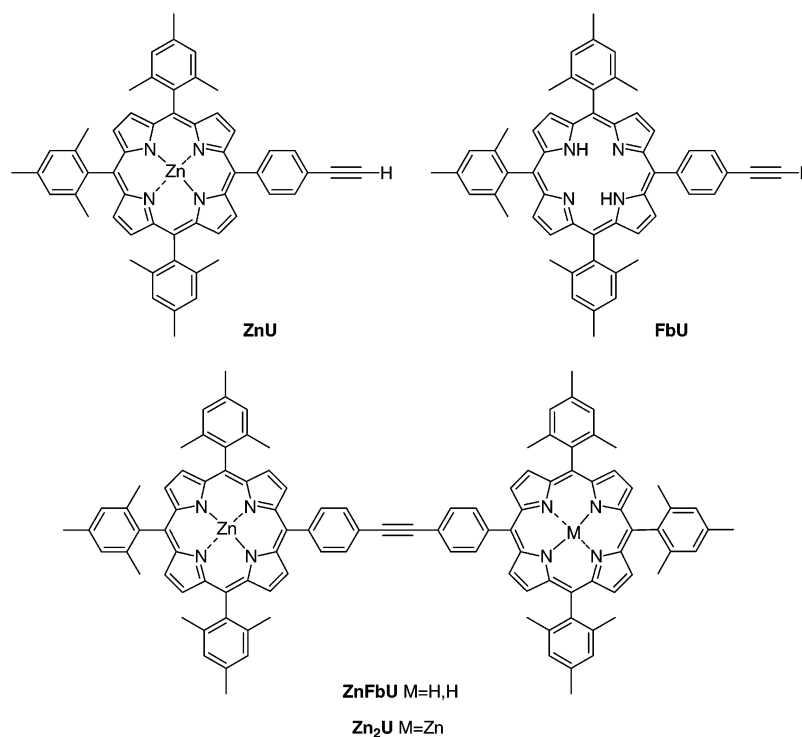| Dyad	Precursors	X	M^1	M^2
ZnFb-dyad	**Zn1 + 2**	CH$_2$	Zn	H, H
Zn$_2$-dyad	**Zn1 + Zn2**	CH$_2$	Zn	Zn
Cu$_2$-dyad	**Cu1 + Cu2**	CH$_2$	Cu	Cu
Oxo-ZnFb-dyad	**Oxo-Zn1 + Oxo-2**	C=O	Zn	H, H
Oxo-Zn$_2$-dyad	**Oxo-ZnFb-dyad**	C=O	Zn	Zn
Oxo-Cu$_2$-dyad	**Oxo-Cu1 + Oxo-Cu2**	C=O	Cu	Cu

iodo/ethyne reactants) at 35 °C in the absence of any copper reagents.[10] Thus, the reaction of **Zn1** and **2** was performed with monitoring by analytical SEC. High molecular weight material and monomer species were removed by chromatography, affording **ZnFb-dyad** in 23% yield. Similar coupling reactions afforded **Zn$_2$-dyad**, **Cu$_2$-dyad**, **Oxo-ZnFb-dyad**, and **Oxo-Cu$_2$-dyad**. The all-zinc array **Oxo-Zn$_2$-dyad** was prepared by the metalation of **Oxo-ZnFb-dyad** (Chart 2).

Electrochemistry of Reference Monomers and Dyads. The redox characteristics of selected free-base chlorin and oxochlorin reference monomers were measured to complement those determined previously for the analogous zinc-containing monomers.[9] These values were determined for reference compounds

(10) Wagner, R. W.; Ciringh, Y.; Clausen, C.; Lindsey, J. S. *Chem. Mater.* **1999**, *11*, 2974−2983.
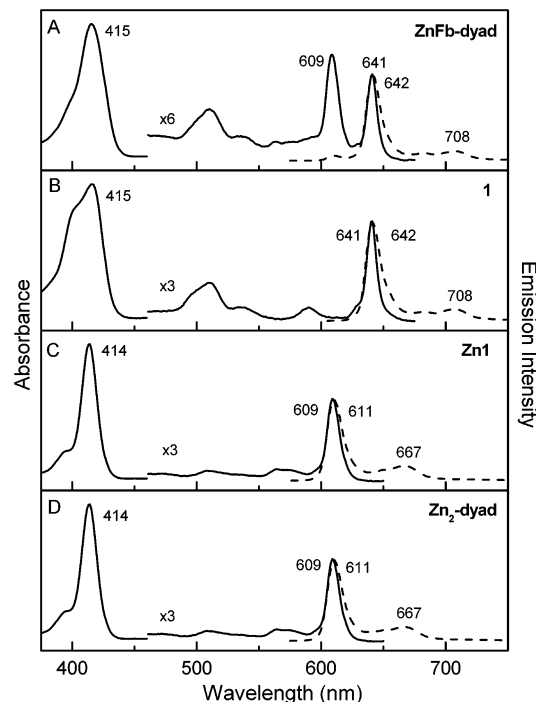
Chart 3

ZnU

FbU

ZnFbU M=H,H
Zn₂U M=Zn

in which the 3,5-di-*tert*-butylphenyl and ethynyphenyl groups of **1**, **Oxo1**, **Zn1**, and **Oxo-Zn1** (Chart 1) are replaced by *p*-tolyl and mesityl groups, respectively.[9] The former replacement has negligible effect on redox potentials, whereas the latter has a minimal effect (on the order of 30 mV).[11] Previously, we determined that the first oxidation potential of a zinc oxochlorin (0.59 V) is more positive by ∼0.24 V than for a zinc chlorin (0.35 V).[9] Herein, we find that the first reduction potential of a free-base oxochlorin (−1.47 V) is less negative by ∼0.16 V than a free-base chlorin (−1.63 V). For comparison, for typical porphyrins such as **ZnU** and **FbU** (Chart 3) the first oxidation potentials[11] are 0.59 and 0.71V, respectively, and the first reduction potentials are −1.76 and −1.61 V (Seth, J.; Diers, J. R.; Bocian, D. F. Unpublished data). All these values were determined in the same solvent (CH₂Cl₂ containing 0.1 M Bu₄-NPF₆) referenced to FeCp₂/FeCp₂⁺ = 0.19 V.

The redox characteristics of the chlorin and oxochlorin dyads were also examined. The potentials of the dyads are essentially identical to those of the reference monomers, indicative of the weak electronic interactions between the constituent chlorin/oxochlorins in the ground electronic state. This behavior is identical to that we previously found for bis-zinc and zinc−free-base porphyrin dyads joined by a diphenylethyne unit.[11]
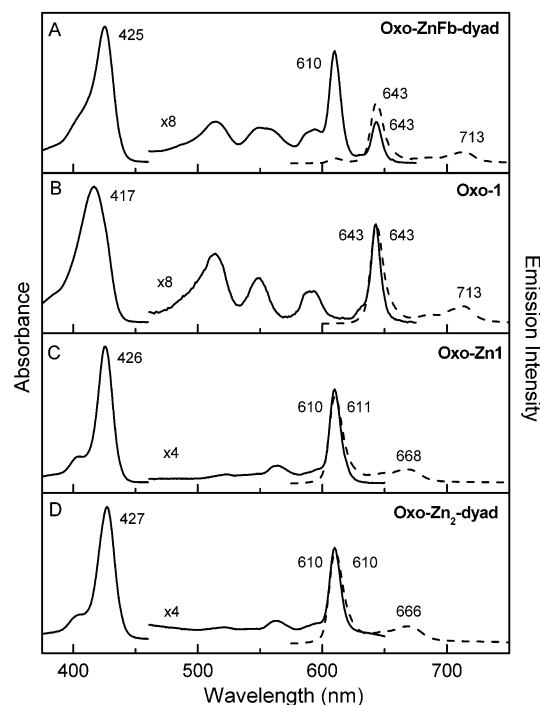
Absorption Spectra of the Dyads. The all-zinc arrays **Zn₂-dyad** and **Oxo-Zn₂-dyad** (Figures 1D and 2D) have virtually the same absorption spectra in toluene as the most relevant reference compounds **Zn1** and **Oxo-Zn1** (Figures 1C and 2C). Similarly, the spectra of the ZnFb arrays **ZnFb-dyad** and **Oxo-ZnFb-dyad** are generally well described by the sum of the spectra of the respective constituent zinc-containing and free-base benchmark compounds, with some deviation due to exciton coupling involving the strong Soret transition dipoles. For

(11) Seth, J.; Palaniappan, V.; Wagner, R. W.; Johnson, T. E.; Lindsey, J. S.; Bocian, D. F. *J. Am. Chem. Soc.* **1996**, *118*, 11194−11207.

Figure 1. Electronic ground-state absorption spectra (solid) and fluorescence spectra (dashed) of chlorin dyads and reference compounds in toluene at room temperature.

example, the spectrum of **ZnFb-dyad** contains the $Q_y(0,0)$ bands of the zinc and free-base components at basically the same positions (∼610 and ∼640 nm) as those of **Zn1** and **1** (Figure 1A−C). The same is true of **Oxo-ZnFb-dyad** compared to its isolated subunits **Oxo-Zn1** and **Oxo-1** (Figure 2A−C). This situation also holds for both dyads in benzonitrile, in which the absorption bands of the zinc-containing components (and

Figure 2. Electronic ground-state absorption spectra (solid) and fluorescence spectra (dashed) of oxochlorin dyads and reference compounds in toluene at room temperature.

reference compounds) are red shifted ∼5 nm from their positions in toluene due to solvent coordination to the metal ion. In general, these findings reflect the relatively weak electronic interactions between the diarylethyne-linked subunits and combined with other observations described below show that the inherent electronic properties designed into the building blocks are largely retained in the dyads.

Fluorescence Properties of the Dyads. The fluorescence spectrum of **Zn$_2$-dyad** in toluene is identical to that of the benchmark compound **Zn1** (Figure 1C and D). The emission spectra of **Oxo-Zn$_2$-dyad** and its reference pigment **Oxo-Zn1** are also the same (Figure 2C and D). These results again reflect the relatively weak electronic coupling between the chromophores in the dyad (in both the ground and excited electronic states).

The fluorescence from **ZnFb-dyad** and **Oxo-ZnFb-dyad** occurs mainly from the free-base unit even when the zinc-containing subunit is preferentially (but not exclusively) excited. For example, emission from **ZnFb-dyad** (Figure 1A, dashed) is dominated by the same $Q_y(0,0)$ band at ∼640 nm present in the spectrum of **1** (Figure 1B) with relatively little of the $Q_y(0,0)$ emission at ∼610 nm characteristic of **Zn1**. The same is true for **Oxo-ZnFb-dyad** compared to its subunits (Figure 2A–C). These results show that the excited Zn–chlorin or Zn–oxochlorin (Zn*) transfers energy efficiently to the Fb–chlorin or Fb–oxochlorin (to produce Fb*) in the respective dyad; this process is denoted Zn*Fb → ZnFb* (Figure 3). As one probe of the energy-transfer efficiency, the integrated amplitude of Fb* emission from **ZnFb-dyad** or **Oxo-ZnFb-dyad** upon excitation of the zinc-containing subunit (average using 562 and 606 nm) was found to be 75 ± 20% of that found using direct excitation of the free base component (509 or 514 nm). Considering experimental error, these estimates are in reasonable
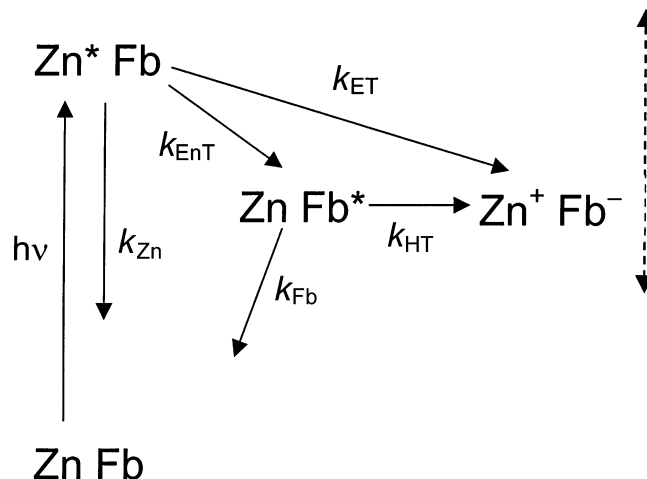
Figure 3. Schematic state diagram showing the likely excited-state processes in the dyads, which include energy transfer (EnT), electron transfer (ET), and hole transfer (HT). The processes labeled k_{Zn} and k_{Fb} include the intrinsic decay processes (fluorescence and internal conversion to the ground state plus intersystem crossing to the excited triplet state) for the respective Zn* and Fb* excited states. The dashed arrow indicates that the (free) energy of the charge-separated state depends on dyad and medium.

agreement with the generally higher energy-transfer yields determined from the time-resolved measurements described below.

The fluorescence yield (±10%) of the free-base component of each dyad in toluene (509–514 nm excitation) was measured relative to the standard value of $\Phi_f = 0.11$ for free-base tetraphenylporphyrin (FbTPP).[12] The yields are $\Phi_f = 0.22$ for **ZnFb-dyad** and $\Phi_f = 0.13$ for **Oxo-ZnFb-dyad** (Table 1). These values are both 20–30% lower than those obtained previously[9,13] for a number of free-base reference compounds of each type such as **1** (0.30) and **Oxo-1** (0.14), respectively. Correspondingly, the fluorescence lifetimes (±5%) of the free-base unit **ZnFb-dyad** (8.1 ns) and **Oxo-ZnFb-dyad** (6.8 ns) in toluene are ∼20% lower than those for free-base reference compounds[9,13] such as **1** (9.6 ns) and **Oxo-1** (8.8 ns), respectively (Table 1). Additionally, in the more polar solvent benzonitrile, the Fb* lifetimes of **ZnFb-dyad** (6.8 ns) and **Oxo-ZnFb-dyad** (5.3 ns) are reduced by ∼20% from the values in toluene, whereas the lifetimes for typical reference compounds[13] are basically solvent independent. These findings indicate that Fb* in each dyad is modestly quenched by charge (hole) transfer to the zinc-containing macrocycle, as described below (Figure 3).

For comparison with the above chlorin and oxochlorin dyads, data on the analogous porphyrin dyad **ZnFbU** (Chart 3) were acquired under the same conditions. The porphyrin dyad shows smaller perturbation of the Fb* lifetime (relative to the isolated chromophore) compared to **ZnFb-dyad** or **Oxo-ZnFb-dyad**. The lifetime for **ZnFbU** in toluene (12.6 ns) is within ∼5% of values found previously for **FbU** and related reference compounds (12.5–13.5 ns).[14–16] The Fb* lifetime for **ZnFbU** is reduced by ∼15% in benzonitrile (11.0 ns), consistent with previous findings[14] for this dyad in other polar media; the

(12) Seybold, P. G.; Gouterman, M. *J. Mol. Spectrosc.* **1969**, *31*, 1–13.
(13) Kirmaier, C.; Hindin, E.; Schwartz, J. K.; Sazanovich, I. V.; Diers, J. R.; Muthukumaran, K.; Taniguchi, M.; Bocian, D. F.; Lindsey, J. S.; Holten, D. *J. Phys. Chem. B* **2003**, *107*, 3443–3454.
(14) Yang, S. I.; Seth, J.; Strachan, J.-P.; Gentemann, S.; Kim, D.; Holten, D.; Lindsey, J. S.; Bocian, D. F. *J. Porphyrins Phthalocyanines* **1999**, *3*, 117–147.

Table 1. Photophysical Properties of Chlorins and Oxochlorins[a]

compound	solvent	Fb unit			Zn unit		
		Φ_f[b]	τ (ns)[c]	Φ_{HT}[d]	τ (ps)[e]	$(k_{EnT})^{-1}$ (ps)[f]	Φ_{EnT}[g]
				dyads			
ZnFb-dyad	toluene	0.22	8.1	0.16	100 ± 10	110 ± 20	0.92
	PhCN		6.8	0.29			
Oxo-ZnFb-dyad	toluene	0.13	6.8	0.23	120 ± 10	140 ± 20	0.80
	PhCN		5.3	0.40	90 ± 10	110 ± 20	0.82
ZnFbU	toluene	0.12[h]	12.6[i]	≤ 0.05	24 ± 2[h]	24 ± 2	0.99
	PhCN		11.0	0.15	26 ± 3[j]	26 ± 3	0.99
				monomers			
1	toluene	0.30[k]	9.6[k,l]				
Zn1		0.085[k]			1400[k,l]		
Oxo-1		0.14[k]	8.8[k,l]				
Oxo-Zn1		0.040[m]			700[n]		
FbU		0.12[o]	13[p]				
ZnU		0.034[q]			2400[q,r]		

[a] All data at room temperature in toluene or benzonitrile (PhCN). [b] Fluorescence quantum yield ($\pm 10\%$). For the dyads, the yield is for the free-base unit using direct Q-band excitation of that subunit. [c] Excited-state lifetime of the free base unit in toluene determined using fluorescence modulation techniques ($\pm 5\%$). [d] Yield of quenching of the excited free-base unit in the dyads as determined from the lifetime in the dyad (τ_{dyad}) and the appropriate reference compound (τ_{ref}) via the formula $\Phi_{HT} = [1 - (\tau_{dyad}/\tau_{ref})]$. [e] Excited-state lifetime of the zinc-containing component, determined using transient absorption spectroscopy for the dyads (± 10 ps for the chlorin and oxochlorin and ± 2 ps for the porphyrin) and fluorescence modulation techniques ($\pm 5\%$) for the monomers. [f] Inverse of the rate constant for Zn*Fb → ZnFb* energy transfer; the error limits encompass the possibility of up to 10% competing electron transfer. [g] Yield of Zn*Fb → ZnFb* energy transfer (± 0.02 for the chlorin and oxochlorin and ± 0.01 for the porphyrin). Up to ~10% of the Zn* decay may occur by competing electron transfer, which will reduce the energy-transfer yield by this factor. [h] From ref 15. [i] Similar values (12.5−13.5 ns) have been measured previously (ref 15). [j] The lifetime is 27 ± 2 ps in pyridine. [k] From ref 9. [l] The lifetimes of **1**, **Zn1**, and **Oxo1** in benzonitrile are assumed to be approximately the same as in toluene since the lifetimes of related oxochlorins are essentially the same in the two solvents (refs 13 and 26). [m] From ref 13. [n] From refs 9 and 26; the lifetime is 0.6 ns in benzonitrile (ref 26). [o] From refs 14 and 15. [p] Lifetimes of 12.5−13.5 ns have been measured previously for FbU in toluene (refs 14 and 15); lifetimes of 12.5−13.7 ns have been measured in a range of polar solvents such as acetone and acetonitrile (ref 15). [q] From ref 16, with similar values reported in refs 14 and 15. [r] The lifetime is 2.0 ns in benzonitrile (ref 16).

lifetime of **FbU** is relatively constant with solvent polarity (12.5−13.7 ns).[14−16] Thus, the porphyrin array shows much less quenching of Fb* than analogous chlorin or oxochlorin dyads.

Given the relatively weak electronic interactions between the subunits in the dyads as indicated by the electrochemical and optical data, the reduced Fb* fluorescence yields and lifetimes in **ZnFb-dyad** and **Oxo-ZnFb-dyad** (relative to the reference compounds) do not involve significant changes in the intrinsic decay rate constants (fluorescence, internal conversion, intersystem crossing) but rather derive mainly from ZnFb* → Zn^+Fb^- hole transfer (Figure 3). [The alternative charge-separated state Zn^-Fb^+ is less likely owing to its higher energy on the basis of redox potentials.] The hole-transfer yield (Φ_{HT}) for each dyad was obtained using standard methods[11,15−17] and the Fb* lifetimes in the dyad (τ_{dyad}) and reference compound (τ_{ref}) via the formula $\Phi_{HT} = [1 - (\tau_{dyad}/\tau_{ref})]$. The values are listed in Table 1. For example, for **ZnFb-dyad**, $\Phi_{HT} = [1 - (8.1/9.6)] = 0.16$ in toluene and $[1 - (6.8/9.6)] = 0.29$ in benzonitrile. Similar results were obtained from the fluorescence yields. The corresponding hole-transfer yields are somewhat larger for **Oxo-ZnFb-dyad** (0.23 in toluene and 0.40 in benzonitrile). On the other hand, there is much less quenching of the free-base excited state for porphyrin analogue **ZnFbU** (≤ 0.05 in toluene and 0.15 in benzonitrile). The greater Fb* hole-transfer yields in the chlorin and oxochlorin dyads versus

the porphyrin array are consistent with the relative energies of the states based on the redox potentials and static optical data described above: Zn^+Fb^- is 0.1−0.2 eV lower for **ZnFb-dyad** and **Oxo-ZnFb-dyad** than for **ZnFbU** while Fb* is 0.05 eV higher. The greater yield for each dyad in the more polar solvent (benzonitrile versus toluene) is attributable mainly to increased energy stabilization of the charge-separated state.

Time-Resolved Absorption Spectra. Figure 4 shows time-resolved absorption spectra and kinetic data for **ZnFb-dyad** in toluene. These data were obtained using primary (but not exclusive) excitation of the zinc-containing component with ~130 fs excitation flashes at 562 nm. The 1-ps spectrum (solid) is dominated by a feature at ~610 nm derived from excitation of the zinc-containing component to produce Zn*. This feature contains both bleaching of the $Q_y(0,0)$ ground-state absorption band and $Q_y(0,0)$ stimulated emission, the latter reflecting emission elicited by the white-light probe pulse that occurs at approximately the same position as the spontaneous fluorescence band (see Figure 1C). The 1-ps spectrum of **ZnFb-dyad** also shows a smaller feature at 645 nm that represents $Q_y(0,0)$ bleaching and stimulated emission associated with Fb* due to direct excitation of the free-base component (rather than the zinc-containing subunit) in a small fraction of the arrays (compare Figures 1B and 4). By 1 ns, the features associated with Zn* have basically decayed and have been replaced with those due to Fb* as a result of Zn*Fb → ZnFb* energy transfer (Figure 4, dashed). On the basis of the apparent residual bleaching at ~610 nm at 1 ns (and at somewhat earlier times) compared to the initial amplitude due to Zn* at 1 ps, the yield of competing Zn* charge-transfer processes such as Zn*Fb → Zn^+Fb^- is $\leq 10\%$ (Figure 3). The lower panel in Figure 4 shows representative kinetic data and a single-exponential fit probing the decay of the 610-nm feature associated with Zn*. Kinetic

(15) (a) Hsiao, J.-S.; Krueger, B. P.; Wagner, R. W.; Johnson, T. E.; Delaney, J. K.; Mauzerall, D. C.; Fleming, G. R.; Lindsey, J. S.; Bocian, D. F.; Donohoe, R. J. *J. Am. Chem. Soc.* **1996**, *118*, 11181−11193. (b) Li, F.; Gentemann, S.; Kalsbeck, W. A.; Seth, J.; Lindsey, J. S.; Holten, D.; Bocian, D. F. *J. Mater. Chem.* **1997**, *7*, 1245−1262.
(16) Tomizaki, K.-Y.; Loewe, R. S.; Kirmaier, C.; Schwartz, J. K.; Retsek, J. L.; Bocian, D. F.; Holten, D.; Lindsey, J. S. *J. Org. Chem.* **2002**, *67*, 6519−6534.
(17) (a) Yang, S. I.; Lammi, R. K.; Seth, J.; Riggs, J. A.; Arai, T.; Kim, D.; Bocian, D. F.; Holten, D.; Lindsey, J. S. *J. Phys. Chem. B* **1998**, *102*, 9426−9436. (b) Prathapan, S.; Yang, S. I.; Seth, J.; Miller, M. A.; Bocian, D. F.; Holten, D.; Lindsey, J. S. *J. Phys. Chem. B* **2001**, *105*, 8237−8248.
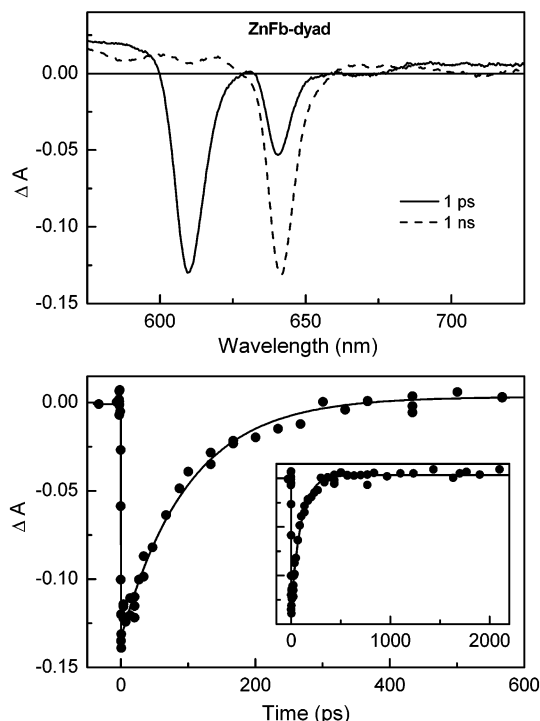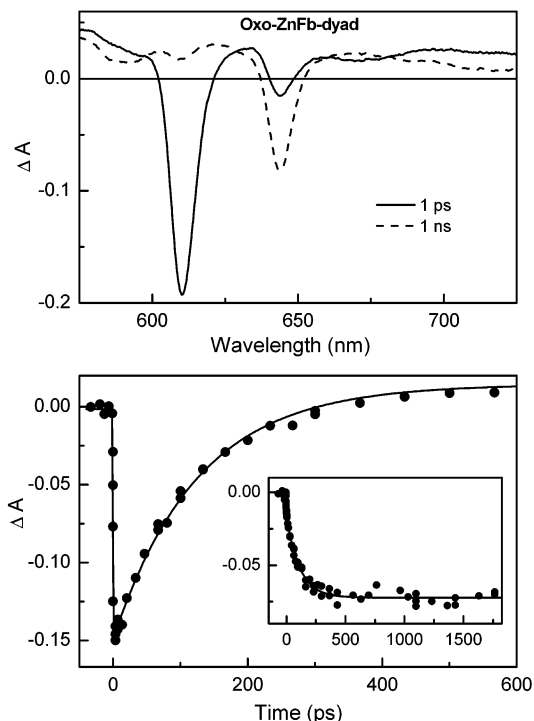
Figure 4. Time-resolved absorption data for **ZnFb-dyad** in toluene at room temperature obtained using 130 fs excitation flashes at 562 nm. The lower panel (with an extended time scale given in the inset) shows kinetic data probing at 609 nm and a fit to a single-exponential function giving a time constant of 100 ± 10 ps. The average Zn* lifetime determined from kinetic traces at this and other wavelengths is given in Table 1.

Figure 5. Time-resolved absorption data for **Oxo-ZnFb-dyad** in toluene at room temperature obtained using 130 fs excitation flashes at 562 nm. The main part of the lower panel shows kinetic data probing at 610 nm and a fit to a single-exponential function giving a time constant of 122 ± 12 ps; the inset shows data and fit for probing at 640 nm giving a time constant of 112 ± 10 ps. The average Zn* lifetime determined from kinetic traces at these and other wavelengths from two independent experiments is given in Table 1.

profiles were analyzed at a number of additional wavelengths including formation of the 645-nm feature derived from Fb*. Collectively, these data give a resultant Zn* lifetime of 100 ± 10 ps for **ZnFb-dyad** in toluene.

The time-resolved absorption spectra for **Oxo-ZnFb-dyad** shown in Figure 5 can be analyzed as described above for **ZnFb-dyad** using the static optical data in Figure 2 as a guide. Kinetic profiles at a number of wavelengths such as those shown in the lower panel of Figure 5 give an overall Zn* lifetime of 120 ± 10 ps for **Oxo-ZnFb-dyad** in toluene. Similar measurements on **Oxo-ZnFb-dyad** in the polar, metal-coordinating solvent benzonitrile (574 nm excitation) give a Zn* lifetime of 90 ± 10 ps. For comparison, studies of the porphyrin dyad **ZnFbU** were carried out in benzonitrile and in pyridine (564 nm excitation) and afford Zn* lifetimes of 26 ± 3 and 27 ± 2 ps, respectively. These values are basically unchanged from that of 24 ± 2 ps obtained for **ZnFbU** in toluene.[15]

Rates and Yields of Energy Transfer. Given the relatively weak interchromophore interactions in the dyads as noted above, we assume that intrinsic decay routes of Zn* (fluorescence, internal conversion, intersystem crossing) are the same as in the reference compounds. Thus, the reduced Zn* excited-state lifetime and fluorescence yield in each dyad versus the reference porphyrin are due to a combination of (1) Zn*Fb → ZnFb* energy transfer with rate constant k_{EnT} and yield Φ_{EnT} and (2) Zn*Fb → Zn$^+$Fb$^-$ electron transfer with rate constant k_{ET} and yield Φ_{ET} (Figure 3). Although we have no clear evidence for Zn* electron transfer in **ZnFb-dyad** and **Oxo-ZnFb-dyad**, any electron transfer is at most a relatively minor pathway ($\Phi_{ET} \leq 0.1$). Such a yield is consistent with (1) the upper limit to this process indicated by the transient absorption data, (2) the static

emission data (using excitation of the zinc versus free base units), and (3) the observed Fb* quenching (presumably by ZnFb* → Zn$^+$Fb$^-$ hole transfer), which indicates that Zn* electron transfer to produce Zn$^+$Fb$^-$ is energetically viable.

To simplify calculations, the energy- and electron-transfer channels are grouped with a combined quenching rate constant k_q and yield Φ_q. These parameters are obtained from the Zn* lifetimes in the dyads (τ_{dyad}) and the reference porphyrins (τ_{ref}) using the standard equations[15−17] $k_q = (\tau_{dyad})^{-1} - (\tau_{ref})^{-1}$ and $\Phi_q = [1 - (\tau_{dyad}/\tau_{ref})]$. Using the lifetimes in Table 1, these equations give $k_q = (100 \text{ ps})^{-1} - (1400 \text{ ps})^{-1} \sim (110 \text{ ps})^{-1}$ and $\Phi_q = [1 - (110/1400)] = 0.92$ for **ZnFb-dyad** in toluene; $k_q \sim (140 \text{ ps})^{-1}$ and $\Phi_q = 0.80$ for **Oxo-ZnFb-dyad** in toluene; and $k_q \sim (110 \text{ ps})^{-1}$ and $\Phi_q = 0.82$ for **Oxo-ZnFb-dyad** in benzonitrile. If Zn* electron transfer is assumed to be negligible, then the energy-transfer parameters are given by $k_{EnT} \sim k_q$ and $\Phi_{EnT} \sim \Phi_q$, and these values are listed in Table 1. An assumption of 10% Zn* electron transfer would give energy-transfer parameters approximated by $k_{EnT} \sim 0.9 \approx k_q$ and $\Phi_{EnT} \sim 0.9 \approx \Phi_q$. The resulting rate constants are within the error limits of those given in Table 1. For comparison, energy-transfer rates and efficiencies for the analogous porphyrin dyad **ZnFbU** obtained previously in toluene ($k_{EnT} = (24 \text{ ps})^{-1}$ and $\Phi_{EnT} = 0.99$)[15] and here in benzonitrile ($k_{EnT} = (26 \text{ ps})^{-1}$ and $\Phi_{EnT} = 0.99$) or pyridine ($k_{EnT} = (27 \text{ ps})^{-1}$ and $\Phi_{EnT} = 0.99$) are given in Table 1. Taken together, these findings show that Zn*Fb → ZnFb* energy transfer is slower and less efficient in the chlorin and oxochlorin dyads than in the porphyrin dyad that incorporates the same diphenylethyne linker.
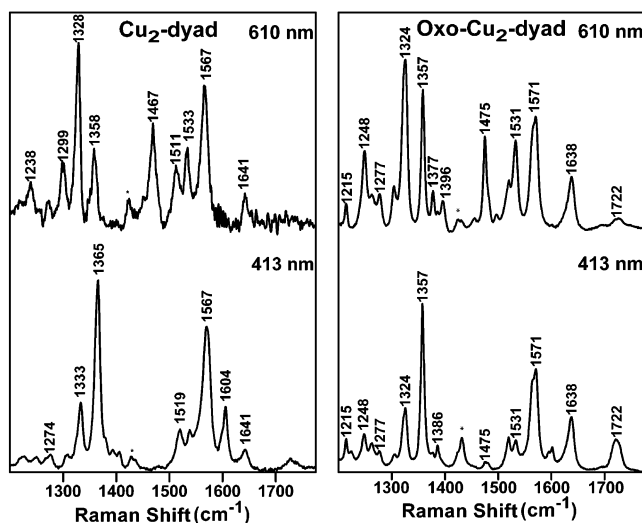
Figure 6. High-frequency regions of the Soret-excitation (λ_{ex} = 413 nm) and Q_y-excitation (λ_{ex} = 610 nm) resonance Raman spectra of **Cu₂-dyad** and **Oxo-Cu₂-dyad**. The bands marked by the asterisk are due to the solvent (CH₂Cl₂).

Resonance Raman Spectra of the Dyads. The high-frequency regions of the Soret-excitation (λ_{ex} = 413 nm) and Q_y-excitation (λ_{ex} = 610 nm) resonance Raman spectra of **Cu₂-dyad** and **Oxo-Cu₂-dyad** are shown in Figure 6. [Note that the resonance Raman spectra were acquired for the Cu complexes because this metal quenches the fluorescence from the Q_y state. This fluorescence compromises the acquisition for Q_y-excitation resonance Raman spectra of Zn and ZnFb complexes.] The spectra for the two dyads are essentially identical to those we have previously reported for similar monomeric chlorins and oxochlorins.[9] The scattering characteristics of all of these chlorins and oxochlorins are also generally similar to those that have been reported for other structurally similar macrocycles.[18,19] In general, the resonance Raman spectra of the chlorins and oxochlorins are much richer than those of porphyrins. This spectral richness arises because of the lower symmetry of the chlorins (and oxochlorins), which results primarily from saturation of one of the β-pyrrole bonds.

A key spectral feature that distinguishes the oxochlorins from the chlorins is the band due to the stretching vibration of the keto group ($\nu_{C=O}$).[19] The $\nu_{C=O}$ mode is observed at ~1722 cm⁻¹ and is strongly resonance enhanced with Soret excitation (Figure 6, right panel, bottom trace). The $\nu_{C=O}$ mode is much less strongly enhanced with Q_y excitation. The relatively weak Q_y enhancement is due to the fact that the keto group of the oxochlorin is at the 17-position, thus lying primarily along the x-axis of the macrocycle (bisecting N-22 and N-24, Chart 1).[18,19] In contrast, the $\nu_{C=O}$ vibration of the keto group of chlorophyll is strongly enhanced with Q_y excitation.[18,19] In the case of chlorophyll, the keto group is not appended to the saturated pyrrole ring of the macrocycle but rather is attached to the 13-position as part of an exocyclic five-membered ring; the keto group thus lies along the y-axis of the chlorophyll chromophore (bisecting N-21 and N-23).

An additional vibrational feature that is observed for **Cu₂-dyad** and **Oxo-Cu₂-dyad** is the stretching vibration of the ethyne group ($\nu_{C\equiv C}$). The $\nu_{C\equiv C}$ mode is observed at ~2215 cm⁻¹ and is only observed with Soret excitation (not shown). This $\nu_{C\equiv C}$ mode is also resonance enhanced in porphyrin dyads joined by a diphenylethyne linker.[11] However, the magnitude of the resonance enhancement for the porphyrin dyads is larger than for the chlorin or oxochlorin dyads. Together these results indicate that the coupling between the π-electron system of the macrocycle and the ethynyl group is weaker for the chlorins and oxochlorins than for the porphyrins. This finding parallels the diminished through-bond excited-state energy-transfer rates for the two hydroporphyrin dyads compared to the porphyrin arrays, as described below.

Förster Energy-Transfer Calculations. The absorption and emission spectra described earlier have been used with standard Förster resonance energy transfer theory (FRET)[20,21] to compute the rates k_{TS}, which are displayed as lifetimes in Table 2. Specifically

$$k_{TS} = 8.785 \cdot 10^{-11} \cdot \frac{\kappa^2}{n^4 R^6} \cdot \frac{\Phi_F}{\tau} \cdot \int_{\Delta\lambda} f_D(\lambda)\lambda^4 \epsilon_A(\lambda)d\lambda \ (\text{ps}^{-1})$$

where κ^2 is a geometrical factor estimated as 1.125,[15] n is the effective index of refraction determining the Coulomb interaction between donor and acceptor,[21] R (nm) is the distance between chromophores, and Φ_F and τ (ps) are the donor fluorescence yield and lifetime, respectively, in the absence of energy transfer. In the spectral-overlap integral, $f_D(\lambda)$ is the donor emission spectrum normalized such that $\int f_D(\lambda) \, d\lambda = 1$, and $\epsilon_A(\lambda)$ is the acceptor absorption spectrum in L/(mol cm). The factor λ^4 is in nm⁴. In Table 2, the spectral-overlap integral is given symbol J with units cm⁶. The overall numerical coefficient accommodates the units of the quantities as specified here. Finally, the range of integration $\Delta\lambda$ is selected simply to cover the region in which the integrand is appreciable, typically from the short-wavelength tail of the emission to the long-wavelength tail of the absorption. Some initial calculations were performed using the program PhotochemCad,[22] with results similar to those given in Table 2.

Key comparisons among the results of the Förster calculations and the experimental rates and yields will be given below. Here we note some differences in the predicted Förster rates for **Oxo-ZnFb-dyad** and **ZnFbU** in benzonitrile versus toluene. These solvents differ in dielectric constant, but more importantly benzonitrile can have a significant effect on the photophysical properties of the zinc-containing components (and reference porphyrins) via axial ligation of the solvent to the central metal ion, as described above and in Tables 1 and 2. In the case of **Oxo-ZnFb-dyad**, benzonitrile decreases the calculated rate by 27% because the donor natural fluorescence rate is 10% smaller, the refractive index factor drops by 8% because of the increase in index, and the donor−acceptor overlap drops by 13% (entries 3 and 4 in Table 2). For the porphyrin analogue **ZnFbU**, benzonitrile shifts the calculated rate in the opposite direction,

(18) (a) Schick, G. A.; Bocian, D. F. *Biochim. Biophys. Acta* **1987**, *895*, 127−154. (b) Boldt, N. J.; Donohoe, R. J.; Birge, R. R.; Bocian, D. F. *J. Am. Chem. Soc.* **1987**, *109*, 2284−2298.
(19) (a) Andersson, L. A.; Loehr, T. M.; Wu, W.; Chang, C. K.; Timkovich, R. *FEBS Lett.* **1990**, *267*, 285−288. (b) Mylrajan, M.; Andersson, L. A.; Loehr, T. M.; Wu, W.; Chang, C. K. *J. Am. Chem. Soc.* **1991**, *113*, 5000−5005.

(20) Förster, Th. In *Modern Quantum Chemistry. Istanbul Lectures. Part III. Action of Light and Organic Crystals*; Sinanoglu, O., Ed.; Academic Press: New York, 1975; pp 183−221.
(21) Knox, R. S.; van Amerongen, H. *J. Phys. Chem. B* **2002**, *106*, 5289−5293.
(22) Du, H.; Fuh, R.-C. A.; Li, J.; Corkan, L. A.; Lindsey, J. S. *Photochem. Photobiol.* **1998**, *68*, 141−142.

Table 2. Förster Energy Transfer: Parameters and Results

entry	model for array	donor	acceptor	solvent	ϵ^a (λ, nm)	$\Phi_f{}^b$	τ (ns)^c	J (cm^6)$^d \times 10^{14}$	$(k_{TS})^{-1}$ calc^e (ps)	Φ_{TS} calc^f	$(k_{EnT})^{-1}$ expt^g (ps)	Φ_{EnT} expt^g
1	**ZnFb-Dyad**	**Zn1**	**1**	toluene	34800 (641)	0.085	1.4	4.5	120	0.92	110 ± 20	0.92 ± 0.02
2	**Zn₂-Dyad**	**Zn1**	**Zn1**	toluene	46900 (609)	0.085	1.4	25	21	0.985^h	n/a	n/a
3	**Oxo-ZnFb-Dyad**	**Oxo-Zn1**	**Oxo-1**	toluene	18000 (643)	0.040	0.7	3.0	190	0.79	140 ± 20	0.80 ± 0.02
4	**Oxo-ZnFb-Dyad**	**Oxo-Zn1**	**Oxo-1**	PhCN^i	18000^j (643)	0.031	0.6	2.7	260	0.70	110 ± 20	0.82 ± 0.02
5	**Oxo-Zn₂-Dyad**	**Oxo-Zn1**	**Oxo-Zn1**	toluene	54000 (610)	0.040	0.7	28	20	0.97^h	n/a	n/a
6	**Oxo-Zn₂-Dyad**	**Oxo-Zn1**	**Oxo-Zn1**	PhCN^i	39000 (614)	0.031	0.6	20	32	0.95^h	n/a	n/a
7	**ZnFbU**	**ZnU**	**FbU**	toluene	7800 (548)	0.035	2.4	2.6	840	0.74	24 ± 2	0.99
8	**ZnFbU**	**ZnU**	**FbU**	PhCN^i	7800^j (548)	0.050	2.0	2.1	660	0.75	26 ± 3	0.99
9	**Zn₂U**	**ZnU**	**ZnU**	toluene	22000 (550)	0.035	2.4	0.7	3400	0.44^h	n/a	n/a
10	**Zn₂U**	**ZnU**	**ZnU**	PhCN^i	18000 (563)	0.050	2.0	2.0	700	0.74^h	n/a	n/a

^{a} Absorption coefficient of the acceptor in L/mol/cm at the indicated wavelength (from refs 6, 9, and 15a, or determined here for **Oxo-Zn1** and **ZnU** in benzonitrile). ^{b} Fluorescence yield of the donor in the absence of the acceptor (from refs 9, 13−15, and 26). ^{c} Excited-state lifetime of the donor in the absence of the acceptor (from refs 9, 13−15, and 26). ^{d} Spectral-overlap integral obtained by numerical integration with a resolution ($\delta\lambda$) of 1 nm (see text for definition). Basically the same values are obtained for the porphyrin reference compounds in which the TMS group on the ethyne is replaced with hydrogen (Chart 3). ^{e} The calculated rate constant for through-space Förster energy transfer. The following parameters were employed: actual distance, R = 2.0 nm; orientation factor, κ^2 = 1.125; refractive index, as appropriate (toluene 1.496, benzonitrile 1.529). ^{f} The Förster energy-transfer efficiency calculated from the formula $\Phi_{TS} = \tau/(k_{TS}^{-1} + \tau)$, where τ is the measured lifetime of the donor in the absence of the acceptor and k_{TS} is a calculated value. ^{g} Same as footnote f except that the measured energy transfer rate constant k_{EnT} from the previous column was used in place of k_{TS}. ^{h} One-way transfer efficiency formally defined as in footnote f, but not directly measurable from lifetimes in symmetric dyads. ^{i} PhCN = benzonitrile. ^{j} Assumed to be the same as for the free-base species in toluene.

namely, a 27% increase (entries 7 and 8). While overlap and refractive-index factors decrease the predicted rate, a substantial increase in the donor's natural fluorescence rate (71%) drives the transfer rate upward on balance. The same trends, but more substantial effects of solvent/ligation, are observed for the analogous Zn₂ dyads (entries 5 versus 6, and 9 versus 10).

Discussion

The significant oscillator strength in the lowest energy absorption of chlorins and oxochlorins results in much greater through-space (TS) electronic interactions between the constituent macrocycles relative to that observed in porphyrin dyads. Indeed, the energy-transfer rates of (110 ps)$^{-1}$ and (140 ps)$^{-1}$ observed for **ZnFb-dyad** and **Oxo-ZnFb-dyad**, respectively, in toluene are comparable (within ∼30%) to the calculated Förster TS rates of (120 ps)$^{-1}$ and (190 ps)$^{-1}$ (entries 1 and 3 in Table 2). In contrast, the measured energy-transfer rate of (24 ps)$^{-1}$ for the porphyrin analogue **ZnFbU** in toluene (Chart 3) is 35-fold greater than the predicted Förster rate (Entry 7). In this latter case, the rate of energy transfer is clearly dominated by an interaction that is more substantial than that given by the porphyrin−porphyrin dipole−dipole coupling. This strong coupling has been attributed to a linker-mediated through-bond (TB) electron-exchange mechanism, owing to the manner in which the observed rate is modulated by porphyrin orbital characteristics (energy orderings, electron-density distributions) and porphyrin-linker steric hindrance and connection motif.[23]

One of the factors that underlies the interchromophore TB coupling in the porphyrin dyad **ZnFbU** is that the HOMO in each macrocycle, namely, the $a_{2u}(\pi)$ orbital, has considerable electron density at the *meso*-carbons to which the diphenylethyne linker is attached. When the HOMO is switched to the $a_{1u}(\pi)$ orbital via fluorination of the nonlinking aryl rings of the macrocycles, the energy-transfer rate drops 10-fold from (24 ps)$^{-1}$ to (240 ps)$^{-1}$.[24] Unlike the a_{2u} orbital, the a_{1u} orbital has negligible electron density at the *meso*-carbon linker sites. In the case of chlorins and oxochlorins, one effect of pyrrole-ring saturation in the macrocycle is to push the a_{1u}-like orbital far

above the a_{2u}-like orbital. As a consequence, the a_{1u}-like orbital is the HOMO and makes a much greater contribution to the wave function of the lowest excited singlet state than for porphyrins. This orbital characteristic of **ZnFb-dyad** and **Oxo-ZnFb-dyad** is expected to give much less TB electron-exchange coupling than in porphyrin analogue **ZnFbU** using the same *meso*-linker motif. The reduced linker-mediated electronic communication in the chlorin and oxochlorin dyads is also evident in the diminished resonance enhancements of the ethyne vibrations of the chlorin and oxochlorin dyads versus the porphyrin dyads.

The above comparisons of the calculated and measured rates of the dyads in toluene indicates that the Förster TS mechanism accounts for at least three-fourths (and perhaps nearly all) of the energy transfer in **ZnFb-dyad** and **Oxo-ZnFb-dyad**, with the remaining smaller fraction involving the TB mechanism (entries 1 and 3 in Table 2). The finding that the predicted TS rate for **Oxo-ZnFb-dyad** in benzonitrile versus toluene drops by 27% (as described above) while the measured rate increases by 20% suggests that there may be a medium-dependent change in the relative TS and TB contributions for this dyad (entries 3 and 4). Some increase in the TB coupling might be expected with benzonitrile because solvent ligation to the central metal ion in the zinc-containing macrocycle should raise the a_{2u}-like orbital and thereby increase electron density at the linker site in the excited-state wave function. The relative contribution of this and other factors such as the LUMOs (in the TB mechanism) and the orientation factor κ^2 (in the TS mechanism) to the solvent/ligation effect for **Oxo-ZnFb-dyad** is unclear at present. Regardless, the results indicate that the TS mechanism makes a contribution at least comparable to that of the TB mechanism for **Oxo-ZnFb-dyad** in benzonitrile. In contrast, the predicted TS rate for the porphyrin dyad **ZnFbU** in benzonitrile, like that in toluene, remains significantly (a factor of 25) less than the measured rate (entries 7 and 8 in Table 2) indicating that the predominance of the TB mechanism in this array is independent of solvent/ligation effects.

Collectively, these findings indicate that the dominant TB coupling in the porphyrin dyad is substantially diminished in the chlorin and oxochlorin dyads, in which the TS interaction makes a major if not the dominant contribution to energy transfer

(23) Holten, D.; Bocian, D. F.; Lindsey, J. S. *Acc. Chem. Res.* **2002**, *35*, 57−69.
(24) Strachan, J.-P.; Gentemann, S.; Seth, J.; Kalsbeck, W. A.; Lindsey, J. S.; Holten, D.; Bocian, D. F. *J. Am. Chem. Soc.* **1997**, *119*, 11191−11201.

depending on array and medium. Thus, k(TS) increases in the series Zn porphyrin−Zn porphyrin < Zn porphyrin−Fb porphyrin < Zn chlorin−Fb chlorin < Zn chlorin−Zn chlorin. Evidently, the enhanced Förster contribution to energy transfer in **ZnFb-dyad** and **Oxo-ZnFb-dyad** (Table 2) is not sufficient to compensate for the attenuated TB contribution (relative to **ZnFbU**), giving an overall 4−5-fold decrease in the energy-transfer rate and a related drop in energy-transfer efficiency (Table 2). The salient point is that a net enhancement in energy-transfer rate derived from increased TS coupling does not necessarily follow from a simple replacement of porphyrins with hydroporphyrins for a given linker architecture. The results obtained herein for one such linker motif indicates that additional design criteria (e.g., shorter linkers, β-linkages) will need to be explored for the ZnFb−chlorins and −oxochlorins to achieve the same rates as the ZnFb porphyrins.

A potential undesirable side effect of the use of simple chlorins or oxochlorins for light-harvesting applications is that excited-state charge-transfer reactions are somewhat more facile than for porphyrins (Figure 3). For **ZnFb-dyad** and **Oxo-ZnFb-dyad,** ZnFb* → Zn⁺Fb⁻ hole transfer that reduces the Fb* lifetime and emission is modest (∼20% in toluene and ∼35% in benzonitrile), while Zn*Fb → Zn⁺Fb⁻ electron-transfer competing with Zn*Fb → ZnFb* energy transfer is generally minor (≤10%). On the other hand, for the porphyrin dyad **ZnFbU** these charge-transfer reactions have much lower yields (generally ≤5% and only ∼15% hole transfer in benzonitrile). A principal reason for the somewhat enhanced charge-transfer processes for the chlorin and oxochlorin dyads is that the Zn⁺Fb⁻ charge-separated states lie 0.1−0.2 eV lower in energy than for the porphyrin analogue due to the differences in redox properties of the chromophores. Charge-transfer quenching of the excited acceptor unit (Fb*), for example, compromises use of the harvested energy for emission or for transfer to a subsequent stage in a larger architecture. However, one should be able to manipulate the redox properties of the chlorins or oxochlorins to raise the energies of the charge-separated states and minimize these unwanted quenching processes.

In addition to the increased red-region absorption and enhanced TS energy transfer of **ZnFb-dyad** and **Oxo-ZnFb-dyad** compared to **ZnFbU**, the TS transfer in **Zn₂-dyad** and **Oxo-Zn₂-dyad** is increased by a factor of 10 in both nonpolar and polar ligating solvents (entries 1 versus 2, 3 versus 5, 4 versus 6 in Table 2). [Such differences between the various Zn₂ and analogous ZnFb dyads in a given solvent can be traced largely to the spectral-overlap integral J listed in Table 2.] As a result, the Zn₂ chlorin and oxochlorin arrays have Förster rates that are ∼170-fold faster than the Zn₂ porphyrin array in toluene and ∼20-fold faster in benzonitrile. Thus, properly designed long linear rods and large branched architectures based on zinc chlorin and oxochlorins that harvest light and transfer the resulting excited-state energy between these units in route to a trap site have advantages compared to the analogous porphyrin systems.

Conclusions

The studies reported herein indicate that while hydroporphyrins display enhanced TS (Förster) electronic coupling, synthetic light-harvesting arrays based on these constructs cannot be implicitly assumed to be more efficient than those based on

porphyrins. Instead, proper synthetic designs will need to take into consideration the unwanted effects that we have uncovered in terms of both energy transfer (reduced TB coupling for the same linkage motif) and excited-state quenching processes. Through proper molecular design, it is likely that these same concepts can be exploited for chlorins and oxochlorins. In this way, the desirable spectral coverage of the latter macrocycles can be combined with proper tuning to yield large arrays that have both superior light harvesting attributes and energy-transfer rates and yields.

Experimental Section

General. All ¹H NMR spectra (300 or 400 MHz) were obtained in CDCl₃ unless noted otherwise. Chlorin and oxochlorin dyads were analyzed by laser desorption mass spectrometry without a matrix (LD-MS) or with the matrix POPOP (MALDI-MS).[25] Fast atom bombardment mass spectrometry (FAB-MS) data are reported for the molecule ion or protonated molecule ion at greater than unit resolution. Column chromatography was performed with flash silica (Baker). Toluene and triethylamine for use in the Pd-mediated coupling process were distilled from CaH₂.

Noncommercial Compounds. Compounds **Zn1**,[8] **Zn2**,[8] and all other chlorins and oxochlorins (**1**, **2**, **Cu1**, **Cu2**, **Oxo-1**, **Oxo-2**, **Oxo-Zn1**, **Oxo-Zn2**, **Oxo-Cu1**, **Oxo-Cu2**)[9] were prepared as described in the literature.

ZnFb-dyad. Following the refined Pd-mediated coupling procedure,[10] samples of **Zn1** (26.5 mg, 38.3 μmol), **2** (28.0 mg, 38.3 μmol), Pd₂(dba)₃ (5.26 mg, 5.75 μmol), and P(o-tol)₃ (14.0 mg, 46.0 μmol) were weighed into a 100-mL Schlenk flask which was then pump-purged three times with argon. Toluene/triethylamine (5:1, 15 mL) was added, and the flask was stirred at 35 °C. Analytical SEC showed that the reaction had leveled off after 5 h. The solvent was removed, and the residue was chromatographed (silica, toluene) affording unreacted chlorin monomers followed by the desired dyad and then high molecular weight material (HMWM). The mixture of dyad and HMWM was concentrated to dryness, dissolved in THF, and chromatographed in four equal portions (SEC, THF) with gravity elution. The dyad-containing fractions were combined and chromatographed (silica, toluene), affording a bluish-purple solid (11.3 mg, 23%): ¹H NMR (toluene-d_8) δ −1.39 to −1.37 (br, 2H), 1.50 (s, 18H), 1.54 (s, 18H), 1.92 (s, 6H), 1.93 (s, 6H), 4.16 (s, 2H), 4.29 (s, 2H), 7.92−7.96 (m, 4H), 7.97−8.03 (m, 4H), 8.11−8.15 (m, 2H), 8.22 (d, J = 2.0 Hz, 2H), 8.29 (d, J = 2.0 Hz, 2H), 8.43 (1H, s), 8.45 (1H, s), 8.56−8.63 (m, 5H), 8.69−8.76 (m, 4H), 8.79−8.81 (m, 1H), 8.83−8.86 (m, 2H), 8.94−8.97 (m, 2H); LD-MS obsd 1293.18, calcd 1292.61 (C₈₆H₈₄N₈-Zn); λ_{abs} 415 (log ϵ = 5.44), 510 (4.24), 609 (4.55), 641 (4.47) nm; λ_{em} 611, 642, 708 nm (Φ_f = 0.22).

Zn₂-dyad. Following the procedure described for the preparation of **ZnFb-dyad**, samples of **Zn1** (13.8 mg, 20.0 μmol) and **Zn2** (15.9 mg, 20.0 μmol) were coupled using Pd₂(dba)₃ (2.75 mg, 3.00 μmol) and P(o-tol) (7.31 mg, 24.0 μmol) in toluene/triethylamine (5:1, 8 mL) at 35 °C under argon. After

(25) (a) Fenyo, D.; Chait, B. T.; Johnson, T. E.; Lindsey, J. S. *J. Porphyrins Phthalocyanines* **1997**, *1*, 93−99. (b) Srinivasan, N.; Haney, C. A.; Lindsey, J. S.; Zhang, W.; Chait, B. T. *J. Porphyrins Phthalocyanines* **1999**, *3*, 283−291.

(26) Muthukumaran, K.; Loewe, R. S.; Kirmaier, C.; Hindin, E.; Schwartz, J. K.; Sazanovich, I. V.; Diers, J. R.; Bocian, D. F.; Holten, D.; Lindsey, J. S. *J. Phys. Chem. B* **2003**, *107*, 3431−3442.

1.5 h, Pd$_2$(dba)$_3$ (2.75 mg, 3.00 μmol) and P(o-tol)$_3$ (7.31 mg, 24.0 μmol) were added to the reaction mixture. Analytical SEC showed that the reaction had leveled off after 2.5 h. Standard workup [(silica, toluene), (SEC, THF) then (silica, toluene)] gave a bluish-purple solid (8.3 mg, 31%): ^{1}H NMR (toluene-d_8) δ 1.53 (s, 36H), 1.87 (s, 12H), 4.16 (s, 4H), 7.92−7.95 (m, 2H), 7.99 (d, J = 8.0 Hz, 4H), 8.13 (d, J = 8.0 Hz, 4H), 8.27−8.29 (m, 4H), 8.42 (s, 2H), 8.45 (s, 2H), 8.55−8.60 (m, 6H), 8.73 (d, J = 4.4 Hz, 2H), 8.84 (d, J = 4.4 Hz, 2H), 8.95 (d, J = 4.4 Hz, 2H); LD-MS obsd 1354.03; FAB-MS obsd 1354.53, calcd 1354.52 (C$_{86}$H$_{82}$N$_8$Zn$_2$); $λ_{abs}$ 414 (log $ε$ = 5.54), 563 (3.45), 609 (4.91) nm; $λ_{em}$ 611, 667 nm ($Φ_f$ = 0.068).

Cu$_2$-dyad. Following the procedure described for the preparation of **ZnFb-dyad**, samples of **Cu1** (8.70 mg, 12.6 μmol) and **Cu2** (10.0 mg, 12.6 μmol) were coupled using Pd$_2$(dba)$_3$ (1.73 mg, 1.89 μmol) and P(o-tol)$_3$ (4.60 mg, 15.1 μmol) in toluene/triethylamine (5:1, 5 mL) at 35 °C under argon. Analytical SEC showed that the reaction had leveled off after 2.5 h. Standard workup [(silica, toluene), (SEC, toluene) then (silica, ethyl acetate)] gave a blue solid (4.3 mg, 25%): LD-MS obsd 1355.41, calcd 1352.54 (C$_{86}$H$_{82}$Cu$_2$N$_8$); $λ_{abs}$ 411 (log $ε$ = 5.23), 500 (3.83), 605 (4.53) nm.

Oxo-ZnFb-dyad. Following the procedure described for the preparation of **ZnFb-dyad**, samples of **Oxo-Zn1** (28.7 mg, 40.6 μmol) and **Oxo-2** (30.2 mg, 40.6 μmol) were coupled using Pd$_2$(dba)$_3$ (5.57 mg, 6.08 μmol) and P(o-tol)$_3$ (14.8 mg, 48.7 μmol) in toluene/triethylamine (5:1, 16 mL) at 35 °C under argon. After 3.5 h, Pd$_2$(dba)$_3$ (5.57 mg, 6.08 μmol) and P(o-tol)$_3$ (14.8 mg, 48.7 μmol) were added to the reaction mixture. Analytical SEC showed that the reaction had leveled off after 4.5 h. Standard workup [(silica, CH$_2$Cl$_2$), (SEC, THF) then (silica, CH$_2$Cl$_2$)] gave a bluish-purple solid (27.8 mg, 52%): ^{1}H NMR (CDCl$_3$) δ −2.36 to −2.33 (br, 1H), −2.22 to −2.19 (br, 1H), 1.52 (s, 18H), 1.54 (s, 18H), 2.06 (s, 6H), 2.06 (s, 6H), 7.78−7.82 (m, 2H), 7.97−8.02 (m, 4H), 8.02−8.07 (m, 4H), 8.17−8.20 (m, 2H), 8.22−8.26 (m, 2H), 8.67−8.72 (m, 4H), 8.87−8.91 (m, 2H), 8.95−8.97 (m, 1H), 8.97−8.98 (m, 2H), 8.99 (1H, s), 9.10−9.12 (m, 1H), 9.19−9.21 (m, 1H), 9.23 (s, 1H), 9.61 (s, 1H), 9.77 (s, 1H); LD-MS obsd 1320.78; FAB-MS obsd 1320.56, calcd 1320.57 (C$_{86}$H$_{80}$N$_8$O$_2$Zn); $λ_{abs}$ 425 (log $ε$ = 5.73), 514 (4.31), 549 (4.24), 594 (4.22), 610 (4.74), 643 (4.31) nm; $λ_{em}$ 643, 713 nm ($Φ_f$ = 0.13).

Oxo-Zn$_2$-dyad. A solution of **Oxo-ZnFb-dyad** (12.0 mg, 9.07 μmol) in 11 mL of CH$_2$Cl$_2$/methanol (1:1) was treated with Zn(OAc)$_2$·2H$_2$O; then the mixture was stirred for 14 h. Standard workup and chromatography [silica, CH$_2$Cl$_2$/hexanes (1:1), ethyl

acetate] gave a bluish-purple solid (4.25 mg, 34%): ^{1}H NMR (toluene-d_8) δ 1.53 (s, 36H), 2.06 (s, 12H), 7.93−7.95 (m, 2H), 7.98 (d, J = 8.0 Hz, 4H), 8.09 (d, J = 8.0 Hz, 4H), 8.26−8.27 (m, 4H), 8.66 (s, 2H), 8.69−8.72 (m, 4H), 8.75 (d, J = 4.8 Hz, 2H), 8.82−8.85 (m, 4H), 9.03 (d, J = 4.8 Hz, 2H), 9.76 (s, 2H); LD-MS obsd 1382.16; FAB-MS obsd 1382.49, calcd 1382.48 (C$_{86}$H$_{78}$N$_8$O$_2$Zn); $λ_{abs}$ 427, 563, 610 nm; $λ_{em}$ 610, 668 nm ($Φ_f$ = 0.041).

Oxo-Cu$_2$-dyad. Following the procedure described for the preparation of **ZnFb-dyad**, samples of **Oxo-Cu1** (8.70 mg, 12.4 μmol) and **Oxo-Cu2** (10.0 mg, 12.4 μmol) were coupled using Pd$_2$(dba)$_3$ (1.70 mg, 1.86 μmol) and P(o-tol)$_3$ (4.53 mg, 14.9 μmol) in toluene/triethylamine (5:1, 5 mL) at 35 °C under argon. After 2.5 h, Pd$_2$(dba)$_3$ (1.70 mg, 1.86 μmol) and P(o-tol)$_3$ (4.53 mg, 14.9 μmol) were added to the reaction mixture. Analytical SEC showed that the reaction had leveled off after 3.5 h. Standard workup [(silica, toluene), (SEC, THF) then (silica, toluene)] gave a blue solid (11.6 mg, 68%): LD-MS obsd 1382.36; FAB-MS obsd 1380.49, calcd 1380.48 (C$_{86}$H$_{78}$Cu$_2$N$_8$O$_2$); $λ_{abs}$ 424 (log $ε$ = 5.68), 561 (4.21), 605 (4.83) nm.

Physical Methods. The electrochemical measurements, static and time-resolved absorption and emission spectroscopy, and resonance Raman spectroscopy were performed as described previously for monomeric chlorin and oxochlorins.[9] This included keeping the absorbance of the long-wavelength band <0.1 (typically ∼0.05) in order to minimize effects emission reabsorption on fluorescence yields and spectra. The absorption coefficients ($ε$) for **Oxo-ZnFb-dyad** and **ZnU** in benzonitrile were determined from the known values in toluene (Table 2) as follows: the solvent was removed from three 3-mL aliquots of a stock solution of the compound (having a measured absorbance spectrum and concentration) in benchtop vacuum centrifuge, 3-mL of benzonitrile added to each dried sample, the absorbance spectra measured, and the resulting three determinations of $ε$ averaged.

Supporting Information Available: Characterization data (^{1}H NMR, LD-MS spectra) for all new dyads. This material is available free of charge via the Internet at http://pubs.acs.org.

JA035987U